

First-principles study of cubic perovskites SrMO₃ (M = Ti, V, Zr and Nb)

I.R. Shein*, V.L.Kozhevnikov and A.L. Ivanovskii

Institute of Solid State Chemistry, Ural Branch of the Russian Academy of Sciences, 620219, Ekaterinburg, Russia

Using the full-potential linearized-augmented-plane-wave (FLAPW) method, we have analyzed systematically the trends in the structural and electronic properties of the 3d and 4d transition-metal oxides SrMO₃ (M = Ti, V, Zr and Nb). The optimized lattice parameters, bulk modules, densities of states, band structures and charge density distributions are obtained and compared with the available theoretical and experimental data. The energy gap between O2p - Md bands increases as the covalency of the system decreases going from 3d to 4d based perovskites. The electron configurations of Sr(Ti,Zr)O₃ and Sr(V,Nb)O₃ usually referred to as d⁰ and d¹ oxides, respectively, differ considerably from these idealized "ionic" configurations, and the deviations increase with increasing of the d-p covalent overlap in the oxides.

* E-mail: shein@ihim.uran.ru

PACS numbers: 71.15.Ap, 72.80.Ga, 62.20.Dc

I. INTRODUCTION

Perovskites SrMO₃ attract much attention from physicists and material scientists because of the unusual combination of their magnetic, electronic and transport properties^{1,2,3,4,5,6}. However, the electronic structure features in these complicated systems are not understood comprehensively yet, and attempts to explain their behavior in different conditions are often based on oversimplified models. Through quite a number of publications are known on strontium oxide perovskites with 3d metals on M sites^{7,8,9,10,11,12,13,14,15,16,17,18,19}, the research focus has long been on strontium titanate, SrTiO₃ - one of the generic representatives of 3d transition-metal oxide perovskites. For instance, the LCAO-based approaches are used in non-self-consistent or self-consistent calculations^{15,16,17}. Recently more accurate self-consistent full-potential LAPW, LMTO, ab-initio pseudopotential band structure calculations are performed^{7,8,9,10,12,18,19}. Some attention is given to the related materials, viz., the 3d¹ metal-like perovskite SrVO₃, solid solutions SrTi_{1-x}V_xO₃, SrVO₃/SrTiO₃ superlattices and heteroepitaxial structures SrVO₃/SrTiO₃/Si^{20,21}. Also, the cubic SrVO₃ is treated as a model system for discussion of orbital fluctuations²² and correlation effects²³. As an example of 4d based perovskites, the cubic SrZrO₃ is studied by the discrete variation (DV) molecular orbital method²⁴ and, recently the band structure calculations are performed¹¹ within the local-density approximation (LDA). Finally, the electronic properties of the ideal cubic SrNbO₃, which may be considered as a prototype of an ample family of perovskite-related layered niobates²⁵, are investigated in work²⁶ by means of LMTO-ASA approach. In this Communication, we report results of a systematic study of electronic properties of perovskite-type 3d and 4d transition-metal oxides SrMO₃ (M = Ti, V, Zr and Nb) by means of the FLAPW method within the generalized gradient approximation (GGA). We have evaluated a number of physical parameters such as optimized crystal structure, bulk modulus, density of

states, band structure and electron density distribution and considered their variations with M-type metal.

II. MODELS AND METHOD

The considered SrMO₃ perovskites are assumed to have ideal cubic structure (s.g. Pm3m) where atomic positions in the elementary cell are M: 1a (0,0,0); O: 3d (0,0,1/2); and Sr: 1b (1/2,1/2,1/2). The electronic configurations are taken Ar3d²4s² for Ti, Ar3d³4s² for V, Kr4d²5s² for Zr, Kr4d³5s² for Nb, Kr5s² for Sr and He2s²2p⁴ for O. Here, the noble gas cores are distinguished from the sub-shells of valence electrons. The equilibrium structural parameters and bulk modules are calculated using the Vienna package WIEN2k, which is an implementation of the hybrid full potential (linear) augmented plane-wave plus local orbitals (L)APW+lo method within the density-functional theory²⁷. The basis set inside each MT sphere is split into core and valence subsets. The core states are treated within the spherical part of the potential only, and are assumed to have a spherically symmetric charge density confined within MT spheres. The valence part is treated with the potential expanded into spherical harmonics up to l = 4. The valence wave functions inside the spheres are expanded up to l = 12. The plane-wave expansion with RMT*KMAX equal to 10 and k sampling with 10*10*10 k-points mesh in the Brillouin zone (BZ) is used. All calculations are carried out with optimized lattice constants. We use the Perdew-Burke-Ernzerhof generalized gradient approximation (GGA)²⁸ for the exchange correlation potentials. Relativistic effects are taken into account within the scalar-relativistic approximation.

The self-consistent calculations were considered to have converged when the difference in the total energy of the crystal did not exceed 0.1 mRy as calculated at consecutive steps. We have adopted the MT radii of 1.7 a.u. for O, 1.8 a.u. for M, and 2.5 a.u. for Sr. The lattice constants and bulk modules are calculated by fitting the total energy versus volume according to the

TABLE I: Calculated and experimental values for the lattice parameters, bulk modulus and its pressure derivative of SrMO₃ (M= Ti, V, Zr and Nb).

Parameters	Lattice lattice (Å)		Bulk modulus B ₀ (GPA)		B ₀ '
	Calcul.	Exper.	Calcul.	Exper.	
SrTiO ₃	3.9456* 3.878 ¹¹	3.905 ³²	167.9* 191 ¹¹	183 ³²	4.56*
SrVO ₃	3.8662*	3.841 ³¹ 3.8425 ³³	182.8*	-	5.11*
SrZrO ₃	4.1794* 4.095 ¹¹	4.109 ³⁵	158.28* 171 ¹¹	150 ³⁴	3.66*
SrNbO ₃	4.0730*	-	170.0*	-	3.71*

* - our FLAPW-GGA data

Murnaghan's equation of state²⁹. The total density of states (DOS) was obtained using a modified tetrahedron method³⁰.

III. RESULTS AND DISCUSSION

The lattice constants of the selected perovskites SrMO₃, where M = Ti, Zr, V and Nb, were calculated under constrain of cubic symmetry. The results and some available experimental and theoretical data are summarized in Table 1. It is seen that for SrTiO₃ and SrZrO₃ the calculated LDA constants¹¹ are smaller compared to experimental ones. The GGA improves the lattice constants over the LDA. In fact, the obtained GGA lattice constants are very close to experimental data; the deviations for SrTiO₃, SrZrO₃ and SrVO₃ achieve only about 1%. The bulk modulus decrease going from SrTiO₃ to SrZrO₃ and from SrVO₃ to SrNbO₃; and B₀ values for metal-like SrVO₃ and SrNbO₃ are higher than for insulating SrTiO₃ and SrZrO₃ perovskites. These trends correlate with changes in the lattice constants.

The dispersion E(k) in the high-symmetry directions in the Brillouin zone are shown in Fig.1 where similarity in the energy bands is evident in the oxide perovskites under study. The general features in the spectra can be specified in more detail with the using of SrTiO₃ as example. The lower bands, which are not shown in Fig.1, contain 12 electrons in Sr4p and O2s semi-core states located about -15.5 eV below the Fermi level.

The upper valence band (VB) with the width of about 4.6 eV is derived mainly from O2p orbitals with some admixture of Ti and Sr states, and it contains 18 electrons. The bottom of the conduction band (CB) is composed mainly of Ti3d t_{2g} and e_g states, and at higher energies the Sr4d - like bands are placed. The valence-band top of SrTiO₃ is composed of O2p orbitals, and it is located at the R point, while the VB maximum at the M point is about 0.09 eV lower than the R. The conduction-band bottom is at the Γ point. The CB minimum at X is by 0.11 eV higher than at the Γ point. Thus the indirect gap between R and Γ points is 1.81 eV, and the direct gap at Γ is 2.16 eV. These features of the band structure agree well with the previous calculations, see Table 2. At the same time the experimentally determined indirect band gap in SrTiO₃ achieves about 3.30 eV, while the direct band gap energy is equal to 3.75 eV^{36,37}. The divergence is related to the well-known underestimation of the band gap values within LDA - based calculation methods that treat electron exchange correlations in an approximate way. Notice, however, that the difference in the calculated values for the direct and indirect gaps equals exactly to the same difference in the experimentally observed band gaps.

The nine occupied bands at the Γ point consist of three triply degenerate levels (Γ₁₅, Γ₂₅ and Γ₁₅) with energies of -2.82, -1.17 and -0.39 eV below E_F, respectively. The splitting of the levels (Γ₁₅ - Γ₂₅) and (Γ₂₅ - Γ₁₅) is due to the crystal field effects and electrostatic interaction between O2p orbitals. The triply (Γ₂₅, +1.81 eV) and the doubly (Γ₁₂, +4.12 eV) degenerate levels in the conduction band originate from t_{2g} (π*) and e_g (σ*) bands of titanium, and they are separated with the energy gap of 2.31 eV.

The calculated total (TDOS) and partial (PDOS) densities of states are shown in Fig.2 within the energy interval [E_F - 6 eV ÷ E_F + 8 eV]. The TDOS is almost entirely composed from the PDOSs for Ti3d and O2p states. The valence TDOS originates predominantly from O2p states, which is consistent with SrTiO₃ being a formal d⁰ system with titanium in 4+ oxidation state. There is also a small contribution in the valence TDOS from strontium 5s states. However, there is a Ti3d PDOS in the occupied energy range due to the hybridization with the O2p states indicating the presence of a covalent bonding. Note also that within the cubic symmetry of SrTiO₃ the hybridization between t_{2g} and e_g states is forbidden, and the orbitals within both bands are degenerate. Nevertheless, because of the Ti-O hybridization the admixture of the both t_{2g} and e_g states to the oxygen 2p bands and also their partial overlapping occur. It is seen from Fig. 2 that the e_g states (directed towards oxygen atoms so that they form σ bonds with respective O 2p orbitals) have lower energy in comparison with Ti t_{2g} states forming π-like bonds with O 2p states.

The TDOS profile is formed basically of four peaks

TABLE II: Calculated and experimental values for the bandwidths (in eV) of SrMO₃ (M= Ti, V, Zr and Nb).

Parameters	SrTiO ₃	SrZrO ₃	SrVO ₃	SrNbO ₃
Valence band	4.59* 4.95 ¹¹	3.86* 4.32 ¹¹	7.18* 7.5 ²³	8.12* 6.12 ²⁶
Conduction band (occupied part)	- -	- -	1.05* 1.1 ²³	1.21* 1.18 ²⁶
Band gap: direct(Γ)	2.16* 2.30 ¹¹ 3.75 ³⁶	3.75* 3.62 ¹¹	1.40*	2.79*
indirect(R- Γ)	1.81* 1.92 ¹¹ 3.25 ³⁶ 3.4 ³⁷	3.30* 3.37 ¹¹ 5.6 ³⁷	1.02*	2.38 2.31 ²⁶

* - our FLAPW-GGA data

* - Experimental data³⁶³⁷

centered at - 3.1, -1.3, + 3.6 and + 5.1 eV. A very flat O2p - like band (along Γ -X-M- Γ , see Fig. 1) is responsible for the highest of them placed at - 3.1 eV. The contribution of Ti3d states is quite small in the peak near -1.3 eV. Therefore the DOS peak at this energy may be attributed to quasi-flat bands originating primarily from non-bonding O2p states. The peaks in CB centered at + 3.6 and + 5.1 eV are formed by significant contributions from t_{2g} and e_g bands of Ti3d states.

The comparison of the band structures of the isoelectronic and isostructural SrTiO₃ and SrZrO₃ shows that the dispersion of the bands in SrTiO₃ is much stronger than in SrZrO₃. For example, the VB bandwidth in SrTiO₃ is about 0.73 eV larger. This means that Ti-O bonds are more covalent than respective bonds between zirconium and oxygen. Another obvious difference is that the band gap (which remains indirect in SrZrO₃; the bottom of the conduction band is located at the Γ point in the cubic BZ while the top of the valence band is at the R point) is about 1.49 eV (45%) larger than that of SrTiO₃. In the case of SrZrO₃ the splitting of the bands ($\Gamma_{15} - \Gamma_{25}$) and ($\Gamma_{25} - \Gamma_{15}$) is about 0.75 and 0.62 eV, respectively.

Band structures for d¹ perovskites SrVO₃ and SrNbO₃ are presented in Fig.1, and band structure parameters are listed in Table 2. The VBs of SrVO₃ and SrNbO₃ consist of completely occupied oxygen 2p bands and partially occupied (V,Nb)3d bands. The electronic states near the Fermi level originate mainly from 3d (t_{2g}) states.

TABLE III: Occupation indices (in e) of M e_g and t_{2g} bands of SrMO₃ (M= Ti, V, Zr and Nb).

Band/system	SrTiO ₃	SrZrO ₃	SrVO ₃	SrNbO ₃
M e_g	0.642*	0.742	0.307	0.533
M t_{2g}	0.473	1.313	0.234	0.791

One can see from Fig.2 that for SrVO₃ and SrNbO₃ there is some contribution of the t_{2g} and e_g bands in the energy intervals from -7.2 to -2.1 eV and from -8.3 to 3.6 eV, respectively, because of the hybridization with O2p states. In the case of SrVO₃ the splitting of the bands ($\Gamma_{15} - \Gamma_{25}$) and ($\Gamma_{25} - \Gamma_{15}$) are about 1.94 and 0.81 eV; for SrNbO₃ these values are about 0.95 and 0.74 eV, i.e. larger than for SrTiO₃ and SrZrO₃, respectively. For SrVO₃ and SrNbO₃ the t_{2g} states are dominant in the vicinity of the Fermi level. The e_g and t_{2g} bands are well separated in the CB, and the maximum of the DOS in the e_g band is centered above the upper band edge of the t_{2g} band. The main weight of t_{2g} and e_g states in SrVO₃ is observed in the energy intervals [1.1 ÷ +1.41 eV] and [+1.38 ÷ +5.8 eV], respectively, while in SrNbO₃ the respective regions are located at [-1.2 ÷ +2.3 eV] and [+1.61 ÷ + 8.5 eV].

The obtained results show that the total density of states at the Fermi level $N_{tot}(E_F)$ in SrVO₃ (1.678 states/eV/cell) is about 20% higher than in SrNbO₃ (1.256 states/eV/cell). The main contribution to $N_{tot}(E_F)$ in both systems originates from the t_{2g} bands, and the $N_{tot}(E_F)$ changes are also controlled by the contributions from t_{2g} states: going from SrVO₃ to SrNbO₃, these contributions decrease rapidly from 1.109 to 0.542 states/eV/cell. In order to illustrate the bonding picture in systems under consideration we have plotted the charge density maps for SrTiO₃ and SrVO₃, Fig. 3. It is seen that the covalent interaction between Ti and O or V and O atoms is very strong.

Finally, the perovskites SrTiO₃ and SrVO₃ (and their 4d analogues) are usually referred to as d⁰ and d¹ oxides in the literature. It is seen, however, from Table 3 that calculated electron configurations (viz., Ti3d^{1.115}, Zr4d^{0.541}, V3d^{2.055} and Nb4d^{1.324}) differ considerably from the idealized "ionic" configurations, and the respective deviations increase with the d-p covalent overlap in the oxides.

IV. CONCLUSIONS

In summary, we have performed FLAPW calculations in order to systematically study ground state properties and electronic structure features in 3d and 4d transition-metal oxides SrMO₃, where M = Ti, V,

Zr and Nb. The energy gap between 2p oxygen and d metal bands increases with the decrease in the covalent p-d overlap. The optimized lattice parameters, bulk modules, densities of states, band structures and charge density distributions are obtained and compared with the available theoretical and experimental data. The analysis of the d band population reveals that the deviation of the d metal electron configurations from

the formal ionic state (d^0 for SrTiO_3 , SrZrO_3 and d^1 for SrVO_3 and SrNbO_3) increases with p-d covalent overlap.

ACKNOWLEDGEMENTS

The work was supported by Russian Academy of Science within the program "Hydrogen energy and fuel elements".

-
- ¹ I.A. Leonidov, V.L. Kozhevnikov, E.B. Mitberg, M.V. Patrakeev, V.V. Kharton, F.M.B. Marques, *J. Mater. Chem.* 11 (2001) 1201.
 - ² K.Y. Hong, S.H. Kim, Y.J. Heo, Y.U. Kwon, *Solid State Commun.* 123 (2002) 305.
 - ³ S. Takeno, T. Ohara, K. Sano, T. Kawakubo, *Surface Interface Anal.* 35 (2003) 29.
 - ⁴ A.A. Yaremchenko, M.V. Patrakeev, V.V. Kharton, F.M.B. Marques, I.A. Leonidov, V.L. Kozhevnikov, *Solid State Sci.*, 6 (2004) 357.
 - ⁵ V.L. Kozhevnikov, I.A. Leonidov, E.B. Mitberg, M.V. Patrakeev, A.N. Petrov, K.R. Poepplmeier, *J. Solid State Chem.*, 172 (2003) 296.
 - ⁶ A.L. Shaula, V. V. Kharton, N.P. Vyshatko, E.V. Tsipis, M.V. Patrakeev, F.M.B. Marques, J.R. Frade, *J. Europ. Ceram. Soc.*, 25 (2005) 489.
 - ⁷ M. Arai, S. Kohiki, H. Yoshikawa, S. Fukushima, Y. Waseda, M. Oku, *Phys. Rev. B* 65 (2002) 085101.
 - ⁸ M. Marques, L.K. Teles, V. Anjos, L. Scolfaro, J.R. Leite, V.N. Freire, G.A. Farias, E.F. da Silva, *Appl. Phys. Lett.* 82 (2003) 3074.
 - ⁹ F. Bottin, F. Finocchi, C. Noguera, *Phys. Rev. B* 68 (2003) 035418.
 - ¹⁰ X.G. Guo, X.S. Chen, Y.L. Sun, L.Z. Sun, X.H. Zhou, W. Lu, *Phys. Lett. A* 317 (2003) 501.
 - ¹¹ E. Mete, R. Shaltaf, S. Ellialt?oglu, *Phys. Rev. B* 68 (2003) 035119.
 - ¹² S.F. Matar, *Prog. Solid State Chem.* 31 (2003) 239.
 - ¹³ S.F. Matar, A. Villesuzanne, V. Uhl, *J. Mater. Chem.* 6 (1996) 1785.
 - ¹⁴ Y. Takahashi, F. Munakata, M. Yamanaka, *Phys. Rev. B* 57 (1998) 15211.
 - ¹⁵ L.F. Mattheiss, *Phys. Rev. B* 6 (1972) 4718.
 - ¹⁶ P. Pertosa, F.M. Michel-Calendini, *Phys. Rev. B* 17 (1978) 2011.
 - ¹⁷ P.G. Perkins, D.M. Winter, *J. Phys. C* 16 (1983) 3481.
 - ¹⁸ O.V. Krasovska, E.E. Krasovskii, V.N. Antonov, *Solid State Commun.* 97 (1996) 1019.
 - ¹⁹ T. Jarlborg, *Phys. Rev. B* 61 (2000) 9887.
 - ²⁰ B.K. Moon, H. Ishiwara, *Appl. Phys. Lett.*, 67 (1995) 1996.
 - ²¹ D.H. Kim, D.W. Kim, B.S. Kang, T.W. Noh, D.R. Lee, K.B. Lee, S.J. Lee, *Solid State Commun.* 114 (2000) 473.
 - ²² E. Pavarini, S. Biermann, A. Poteryaev, A. I. Lichtenstein, A. Georges, O.K. Andersen, *Phys. Rev. Lett.* 92, (2004).176403 (2004).
 - ²³ I.A. Nekrasov, G. Keller, D.E. Kondakov, A.V. Kozhevnikov, Th. Pruschke, K. Held, D. Vollhardt, V.I. Anisimov, arXiv:cond-mat/0501240 (2005).
 - ²⁴ M. Yoshino, K. Nakatsuka, H. Yukawa, M. Morinaga, *Solid State Ionics* 127 (2000) 109.
 - ²⁵ F. Lichtenberg, A. Herrnberger, K. Wiedenmann, J. Mannhart, *Prog. Solid State Chem.* 29 (2001) 1.
 - ²⁶ S.A. Turzhevsky, D.L. Novikov, V.A. Gubanov, A. J. Freeman, *Phys. Rev B* 50 (1994) 3200.
 - ²⁷ P. Blaha, K. Schwarz, G.K.H. Madsen, D. Kvasnicka, J. Luitz, WIEN2k, An Augmented Plane Wave Plus Local Orbitals Program for Calculating Crystal Properties, Vienna University of Technology, Vienna, 2001
 - ²⁸ J.P. Perdew, K. Burke, M. Ernzerhof, *Phys. Rev. Lett.*, **77**, (1996) 3865.
 - ²⁹ F.D. Murnaghan, *Proc. Natl. Acad. Sci. U.S.A.* 30 5390 (1944).
 - ³⁰ P.E. Blochl, O. Jepsen, O.K. Anderson, *Phys. Rev. B* 49 16223 (1994).
 - ³¹ M. J. Rey, Ph. Dehaudt, J. C. Joubert, B. Lambert-Andron, M. Cyrot, F. Cyrot-Lackmann, *J. Solid State Chem.* 86 (1990) 101.
 - ³² Numerical Data and Functional Relations in Science and Technology-Crystal and Solid State Physics (Eds. by T. Mitsui, S. Nomura), Landoldt-Bornstein, New Series, Group III, Vol. 16, Springer-Verlag, Berlin, 1982.
 - ³³ Y.C. Lan, X.L. Chen, A. He, *J. Alloys Comp.* 354 (2003) 95.
 - ³⁴ D. de Ligny, P. Richet, *Phys. Rev. B* 53 (1996) 3013.
 - ³⁵ A.J. Smith, A.J.E. Welch, *Acta Crystallogr.* 13, 653 1960.
 - ³⁶ K. van Benthem, C. Elsasser, R.H. French, *J. Appl. Phys.* 90 (2001) 6156.
 - ³⁷ Y.S. Lee, J.S. Lee, T.W. Noh, D.Y. Byun, K.S. Yoo, K. Yamaura, E. Takayama-Muromachi, *Phys. Rev. B* 67 (2003) 113101.

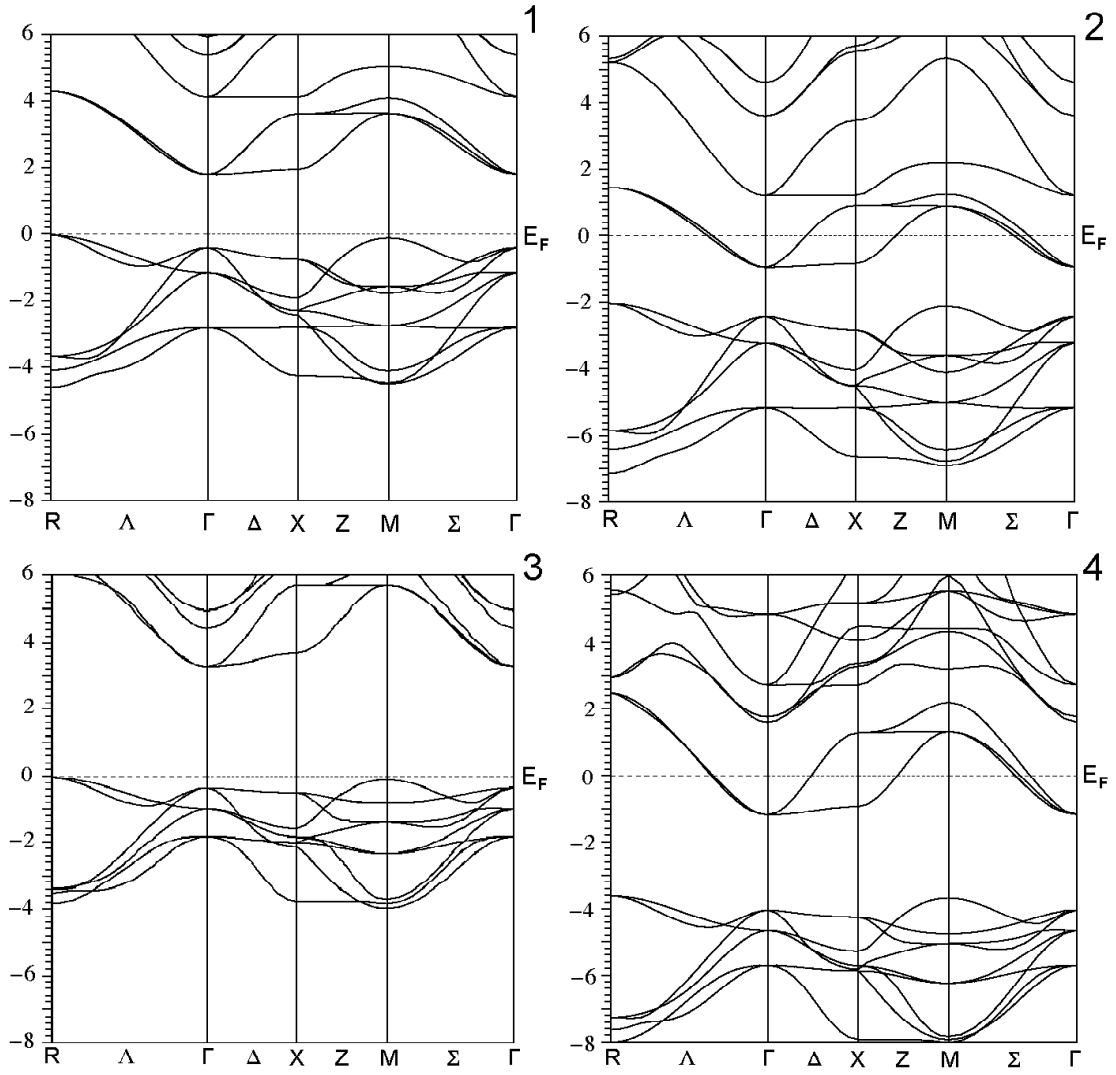


FIG. 1: Band structures of cubic perovskites: 1- SrTiO₃ 2- SrVO₃ 3- SrZrO₃, 4- SrNbO₃. The Fermi level corresponds to 0.0 eV.

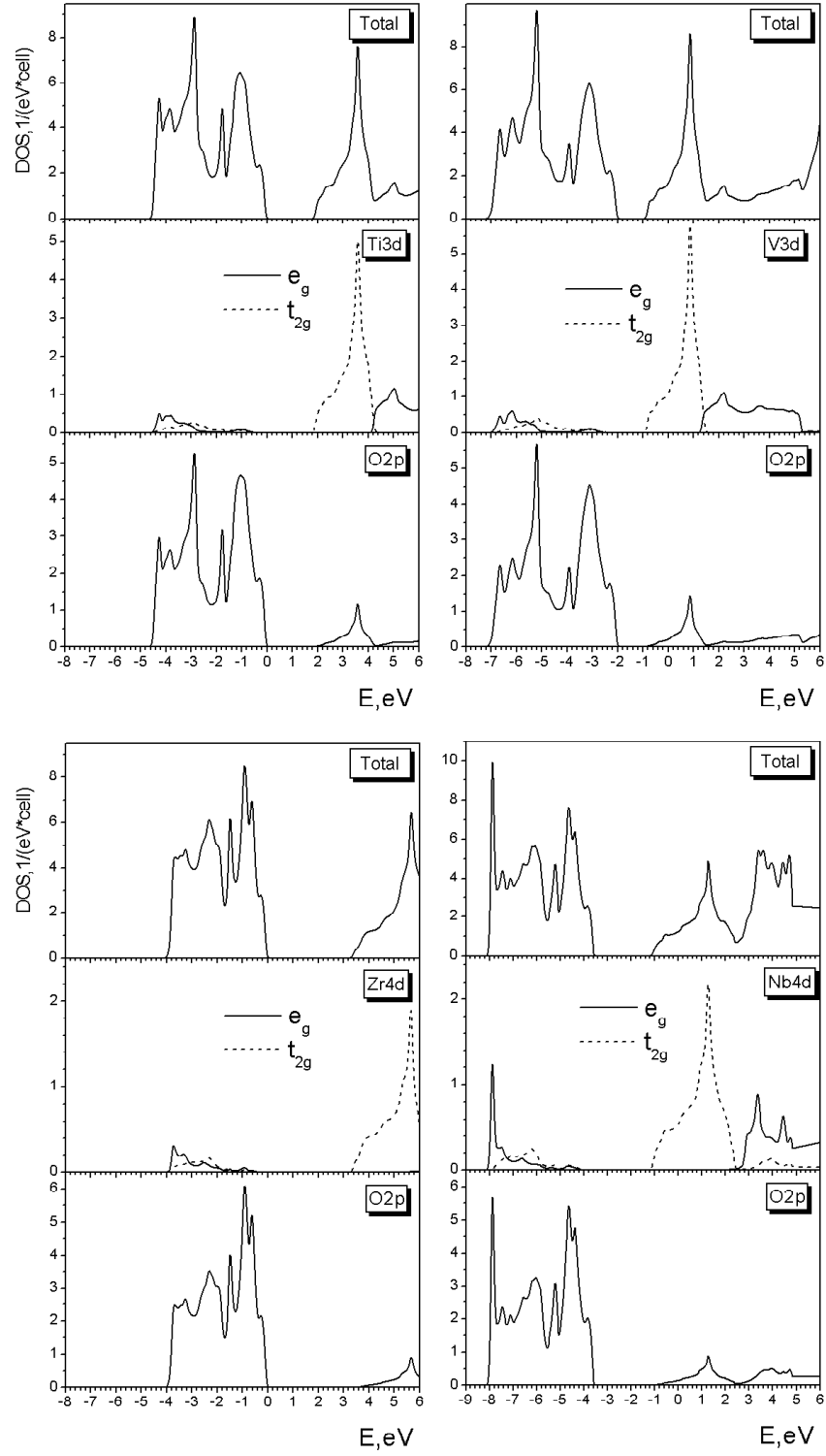


FIG. 2: Total and projected DOSs for the cubic perovskites SrBO_3 ($B = \text{Ti, V, Zr}$ and Nb).

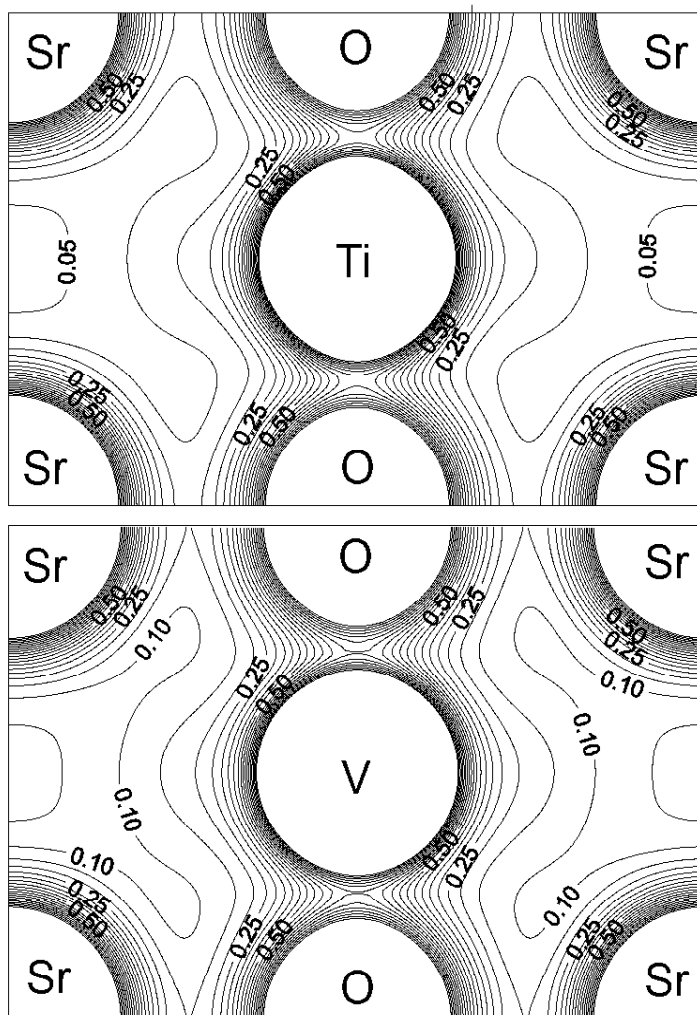


FIG. 3: Charge densities maps for SrTiO₃ and SrVO₃ in (100) plane.